BMC Pulmonary Medicine

RESEARCH

Open Access

ARID1A silencing-mediated upregulation of microRNA-652 accelerates cigarette smoke-induced human bronchial epithelial cell transformation by targeting ZFAND5

Kang-liang Zhang[1], Dan-ni Wu[2], Rui-heng Chen[2], Chong Zheng[2], Ri-sheng Huang[2*] and Xiao-dan Zhao[3*]

Abstract

Cigarette smoking is an important risk factor in lung cancer development. As a class of regulatory RNAs, microRNAs (miRs) participate in various biological processes. In the present study, we searched for the key miRs that mediate cigarette smoke-induced aggressive phenotype in human bronchial epithelial (HBE) cells. Our results demonstrated that miR-652 was upregulated in cigarette smoke extract (CSE)-exposed HBE cells. *ARID1A* silencing due to hypermethylation of its promoter accounted for the upregulation of miR-652 in CSE-treated HBE cells. Overexpression of miR-652 accelerated the proliferation, migration, and anchorage-independent growth of HBE cells exposed to CSE. Knockdown of miR-652 attenuated the growth and migration of CSE-treated HBE cells. According to bioinformatic prediction and luciferase reporter assays, ZFAND5 was found to be a target of miR-652. Overexpression of miR-652 suppressed the protein expression of ZFAND5 in HBE cells, without altering its mRNA abundance. CSE treatment reduced the protein expression of ZFAND5 in HBE cells. Depletion of ZFAND5 potentiated the anchorage-independent growth and migration of CSE-treated HBE cells. Enforced expression of ZFAND5 reversed miR-652-mediated enhancement of anchorage-independent growth and migration in CSE-treated HBE cells. In conclusion, miR-652 potentiates CSE-induced aggressive phenotype in HBE cells by repressing ZFAND5 protein expression. The potential involvement of miR-652 in cigarette smoking-related lung carcinogenesis warrants further investigation.

Keywords Cigarette smoking, Lung epithelial cell, miR-652, Transformation, ZFAND5

*Correspondence:
Ri-sheng Huang
hrs9900@wmu.edu.cn
Xiao-dan Zhao
hlbzxd0506@163.com
[1]Department of Central Lab, The Dingli Clinical College of Wenzhou Medical University, Wenzhou Central Hospital, Wenzhou, China
[2]Department of Thoracic Surgery, The Dingli Clinical College of Wenzhou Medical University, Wenzhou Central Hospital, Wenzhou, China
[3]Department of Nursing, The Dingli Clinical College of Wenzhou Medical University, Wenzhou Central Hospital, Wenzhou, China

Introduction

Lung cancer is a leading cause of cancer-related deaths worldwide [1]. Cigarette smoking is a main risk factor for lung cancer [2]. Over 60 carcinogens have been detected in cigarette smoke [3]. Benzo(a)pyrene (BaP) and nitrosamine are the well-defined tobacco carcinogens with the ability to cause DNA damage and induce lung cancer [4]. Identification of the key factors involved in cigarette smoke-induced lung carcinogenesis is important for the prevention of this malignant disease.

microRNAs (miRs) are a class of endogenous small non-coding RNAs of approximately 22 nucleotides in length. They are evolutionarily conserved and can elicit posttranscriptional regulation of gene expression via incomplete base pairing to the 3′-untranslated region (UTR) of target mRNAs [5]. miRs are involved in various biological processes including cell proliferation, survival, migration, invasion, inflammation, and tumorigenesis [6]. A number of miRs have been found to mediate cigarette smoke-induced cancer development and progression [7]. For instance, cigarette smoke provokes miR-25-3p production to enhance the proliferation and invasion of pancreatic cancer cells [7]. Another study has reported that cigarette smoke exposure leads to epigenetic silencing of miR-487b, a tumor suppressor in lung cancer cells [8]. Besides the regulation of miRs in cancer cells, cigarette smoke also affects the expression of miRs in non-malignant cells [9, 10]. Several miRs such as miR-217, miR-218, and miR-200c have been found to be downregulated by cigarette smoke extract (CSE) in human bronchial epithelial (HBE) cells [10–13]. Interestingly, epigenetic silencing of miR-218 leads to increased self-renewal and malignancy in CSE-treated HBE cells [11]. These studies suggest that miR regulators play an important role in cigarette smoke-induced carcinogenesis.

In the present study, we identified miR-652 as a novel key mediator of CSE-induced aggressive phenotype in HBE cells. Unlike miR-217, miR-218, and miR-200c, the expression of miR-652 was upregulated in HBE cells exposed to CSE. Epigenetic silencing of AT-interacting domain-rich protein 1 A (ARID1A) led to the upregulation of miR-652 in CSE-treated HBE cells. ARID1A is a subunit of the switch/sucrose non-fermentable (SWI/SNF) chromatin remodeling complex, which alters chromatin structure and DNA accessibility to modulate gene transcription [14]. ARID1A functions as a tumor suppressor, and its loss contributes to cancer development and progression [15, 16]. We demonstrated that overexpression of miR-652 enhanced the proliferation, anchorage-independent growth, and migration of CSE-exposed HBE cells. Hence, miR-652 may act as a potential target for the prevention of cigarette smoke-related neoplastic transformation in human lung epithelial cells.

Materials and methods

Cell culture

HBEC3-KT bronchial epithelial cells were purchased from the American Type Culture Collection (ATCC, Manassas, VA, USA). The cells were cultured in the Airway Epithelial Cell Basal Medium supplemented with Bronchial Epithelial Cell growth Kit (ATCC, Manassas, VA, USA). HEK293 cells were cultured in RPMI-1640 medium (Lonza, Basel, Switzerland) supplemented with 10% foetal bovine serum (FBS; Sigma-Aldrich, St. Louis, MO, USA). Routine laboratory testing indicated no mycoplasma contamination.

CSE preparation and cell treatment

CSE was prepared as described previously [17]. In brief, the condensate from smoking 3R4F Kentucky Research cigarettes (University of Kentucky, Lexington, KY, USA) was collected using a glass fibre filter. Weight increase for the filter indicated the amount of total particulate matter. The cigarette smoke particulates trapped on the filter were sequentially extracted using dimethyl sulfoxide (DMSO) and culture medium. The DMSO (for water-insoluble components) and culture medium (for water-soluble components) extractions were mixed to generate the total CSE solution. The CSE was freshly prepared before use.

To induce HBE cell malignant transformation, HBEC3-KT cells were exposed to 10 μg/mL CSE for 1 or 4 weeks [17]. The cell medium containing CSE was refreshed every 3–4 days. In some experiments, CSE-exposed HBEC3-KT cells were treated with 10 μM 5-azacytidine (Sigma-Aldrich) [18] for 24 h before analysis of gene expression. The cell culture medium was used as the control for CSE and 5-azacytidine.

RNA extraction and quantitative real-time PCR (qRT-PCR) analysis

Total RNA was extracted using Trizol reagent (Thermo Fisher Scientific, Waltham, MA, USA) and reverse-transcribed to cDNA using the first-strand synthesis system (Thermo Fisher Scientific) according to the manufacturer's instructions. The transcripts *ARID1A* and *ZFAND5* were measured by qRT-PCR analysis using the following primers: *ARID1A* forward 5′-CCTGAAGAACTCGAACGGGAA-3′, *ARID1A* reverse 5′-TCCGCCATGTTGTTGGTGG-3′; *ZFAND5* forward 5′-GAGCCCTCGGACTCCATCACT-3′, *ZFAND5* reverse 5′-AGGCAGAGGCAGGAGAATCAC-3′. The relative gene expression was calculated by normalizing against the level of *GAPDH*.

For measurement of miR expression, the All-in-One miRNA First-Strand cDNA Synthesis Kit (GeneCopoeia, Guangzhou, China) was used. According to the manufacturer's instructions, mature miRs were polyadenylated by poly(A) polymerase and then subjected to cDNA

synthesis. qRT-PCR was performed using the All-in-One miRNA qPCR Kit (GeneCopoeia) with miR-specific primers and universal reverse primers (Supplementary Table S1). Relative miR levels were determined after normalization to the endogenous control U6 snRNA.

Methylated DNA immunoprecipitation assay

As described previously [19], methylated DNA immunoprecipitation assay was performed to assess the methylation level at the promoter of *ARID1A*. In brief, genomic DNA fragments from CSE-exposed HBEC3-KT cells was denatured at 95 °C for 10 min and subjected to immunoprecipitation using anti-5-methylcytosine antibody (clone D3S2Z, catalog no. 28692; Cell Signaling Technology, Danvers, MA, USA). The DNA-antibody mixture was incubated overnight at 4 °C. Proteinase K was added to release methylated DNA fragments from the DNA-antibody complex. Quantitative PCR was performed to analyze methylated *ARID1A* sequence using the following primers: forward, 5′-AGGGGACAGACCTGGATA GGG-3′; reverse, 5′-TCAGCACTGCCATTTTACCCA G-3′. An unmethylated sequence, which was used as a normalization control, was also analyzed by PCR using the following primers: forward, 5′-GAGAGCATTAGGG CAGACAAA-3′; reverse, 5′-GTTCCTCAGACAGCCA CATTT-3′.

Plasmids, oligonucleotides, and transfection

Two independent *ARID1A* short hairpin RNAs (shRNAs) were cloned into the pLKO.1 puro vector (Sigma-Aldrich), as described previously [20]. The target sequences for *ARID1A* shRNAs are as follows: shARID1A#1: 5′-TAATGCCTTGCCCAATGCCA A-3′; shARID1A#2: 5′-ACATGACCTATAATTATGCC A-3′. The sequences of *ZFAND5*-targeting siRNAs were as follows: si*ZFAND5*#1: 5′-AAUGGAAUGUGUU-CAGUUUtt-3′; si*ZFAND5*#2: 5′-UGAACUUGUU-CAAGUGAUAtt-3′. For overexpression studies, *ARID1A* and *ZFAND5* cDNAs were cloned to pcDNA3.1(+) vector (Thermo Fisher Scientific). miR-652 mimic (MC12699) and anti-miR-652 inhibitor (MH12699; Thermo Fisher Scientific) were used in this study. Cell transfections were conducted using Lipofectamine 3000 (Invitrogen, Carlsbad, CA, USA).

Soft agar assay

HBEC3-KT cells were treated with CSE for indicated times and tested for clonogenic potential by soft agar assays. The 0.6% agar in EMEM was placed to 12-well plates and allowed to solidify. 800 viable cells were suspended in 0.4% agar in EMEM and seeded on the bottom agar layer. After 2 weeks of culture, the colonies were photographed and counted.

Cell proliferation assay

CSE-transformed HBEC3-KT cells were transfected with indicated constructs and seeded on 96-well plates. After culturing for 1, 3, or 5 days, the number of viable cells was determined using the MTT Cell Proliferation Kit (Sigma-Aldrich). Absorbance was measured at a wavelength of 570 nm.

Transwell migration assay

The migratory capacities of HBEC3-KT cells after indicated treatments were determined by Transwell migration assays using a Boyden chamber with an 8-μm-pore filter membrane. Briefly, cells (1×10^4) in the Airway Epithelial Cell Basal Medium were seeded in the upper chamber. The lower chamber was filled with the culture medium containing 10% FBS. After incubation for 24 h, the cells that migrated to the lower chamber were stained with crystal violet and counted.

Luciferase reporter assay

The luciferase reporter constructs were prepared by inserting the 3′-UTR of *ZFAND5*, *ISL1*, *TNRC6A*, *NPTN*, or *CAPZB* into pGL3 Luciferase Reporter Vector (Promega Corporation, Madison, WI, USA). To disrupt the putative miR-652 binding site in the 3′-UTR of *ZFAND5*, site-directed gene mutagenesis was performed using the QuickChangeXL Site-Directed Mutagenesis Kit (Stratagene, La Jolla, CA, USA) following the manufacturer's instructions. The reporter constructs were co-transfected to HEK293 cells using Lipofectamine 3000, together with miR-652 mimic or negative control mimic (miR-NC). The pRL-CMV vector (Promega) that expresses *Renilla* luciferase was used as an internal control. After culturing for 24 h, the cells were lysed and examined for luciferase activities using the Dual-luciferase Reporter Assay Kit (Promega).

Western blot analysis

Cells were lysed in ice-cold lysis buffer containing protease and phosphatase inhibitors (Sigma-Aldrich). Protein concentrations were determined using a BCA Protein Quantification kit (Beyotime, Shanghai, China). Protein samples were resolved by sodium dodecyl sulfate-polyacrylamide gel electrophoresis and transferred onto a polyvinylidene difluoride (PVDF) membrane. The membrane was incubated with anti-ZFAND5 (clone OTI1D8, catalog no. MA5-26455), anti-ARID1A (clone GT3611, catalog no. MA5-27793), or anti-GAPDH (clone 4A9L6, catalog no. MA5-35235) antibodies (Thermo Fisher Scientific) at 4 °C overnight, followed by incubation with horseradish peroxidase-conjugated secondary antibodies (Thermo Fisher Scientific) at room temperature for 1 h. Protein signals were detected using the Chemiluminescent Western Blot Detection Kit (catalog no. 32109;

Thermo Fisher Scientific). The band intensities were quantitated using the ImageJ program (National Institutes of Health, Bethesda, Maryland, USA).

Statistical analysis

The data were expressed as the mean ± standard deviation. Statistical difference was assessed using the Student's *t*-test or one-way analysis of variance. A *P* value less than 0.05 was considered statistically significant.

Results

miR-652 is induced in HBE cells exposed to CSE

Analysis of 2 Gene Expression Omnibus (GEO) datasets (GSE175462 and GSE107962) revealed 13 common miRs that were dysregulated both in lung adenocarcinoma samples (relative to adjacent lung tissues) and in lung tissues from mice exposed to cigarette smoke (Fig. 1A). These miRs are listed as follows: miR-1976, miR-1468, miR-3615, miR-552, miR-652, miR-2110, miR-5698, miR-1258, miR-1248, miR-1299, miR-1262, miR-934, and miR-1301. We examined their expression in HBE cells exposed to CSE. miR-652 was significantly induced after CSE treatment, while the other miRs tested remained unchanged (Fig. 1B).

Epigenetic silencing of *ARID1A* contributes to miR-652 upregulation upon CSE exposure

ARID1A is a core component of the mammalian SWI/SNF complex and regulates the expression of a number of target genes [14, 15]. Our previous studies have indicated that *ARID1A* loss induces prolyl 4-hydroxylase subunit beta (P4HB) and plasminogen activator urokinase (PLAU) expression in lung cancer cells [20, 21]. Therefore, we checked whether ARID1A was involved in CSE-induced miR-652 upregulation. Notably, ARID1A expression was reduced in HBE cells after CSE treatment (Fig. 2A). Such reduction was rescued by the DNA demethylating agent 5-azacytidine (Fig. 2A). Methylated DNA immunoprecipitation assays confirmed that CSE treatment led to hypermethylation at the promoter of *ARID1A* (Fig. 2B). Knockdown of ARID1A promoted the expression of miR-652 in HBE cells (Fig. 2C and D), whereas overexpression of ARID1A inhibited the expression of miR-652 in HBE cells (Fig. 2E and F). Additionally, CSE-induced upregulation of miR-652 was impaired by overexpression of ARID1A (Fig. 2F). These results collectively indicate that CSE induces the expression of miR-652 through epigenetic silencing of *ARID1A*.

miR-652 mediates CSE-induced anchorage-independent growth and migration in HBE cells

Chronic treatment with CSE alone has been shown to promote malignant transformation in HBE cells [13, 22]. Thus, we investigated the role of miR-652 in CSE-induced malignant transformation of HBE cells. Soft agar assays were conducted to assess the anchorage-independent growth of HBE cells, a hallmark feature of carcinogenesis [22]. After the 4-week treatment with CSE, HBE cells acquired the ability to form colonies in soft agar (Fig. 3A and B). Notably, miR-652-overexpressing HBE cells formed more colonies after CSE treatment (Fig. 3A and B). Moreover, CSE-induced HBE cell proliferation (Fig. 3C) and migration (Fig. 3D and E) were potentiated by miR-652 overexpression. In contrast, knockdown of miR-652 impaired the proliferation, migration, and anchorage-independent growth of HBE cells after CSE treatment (Fig. 4). These data suggest that miR-652 plays an indispensable role in CSE-induced malignant transformation of HBE cells.

miR-652 represses the expression of ZFAND5 in HBE cells

Both miRDB and TargetScan programs have been widely used to predict target genes for the miRs of interest [23]. According to the 2 prediction algorithms, ISL1, TNRC6A, NPTN, ZFAND5, and CAPZB were potential targets for miR-652. Luciferase reporter assays were performed to check whether miR-652 can modulate the expression of these potential targets. As shown in Fig. 5A, miR-652 overexpression suppressed the expression of the luciferase constructs containing the 3′-UTR of *ZFAND5*, but not *ISL1*, *TNRC6A*, *NPTN*, or *CAPZB*. Mutation of the predicted miR-652 binding site in the 3′-UTR of *ZFAND5* disrupted miR-652-mediated repression of the luciferase reporter (Fig. 5B and C). We next examined the effect of miR-652 on the endogenous expression of ZFAND5 in HBE cells. Overexpression of miR-652 led to a reduction in the ZFAND5 protein level in HBE cells, without altering the mRNA abundance of *ZFAND5* (Fig. 5D and E). Knockdown of miR-652 caused a marked increase in the protein level of ZFAND5 (Fig. 5E). These results indicate that miR-652 post-transcriptionally regulates ZFAND5 expression in HBE cells. Given the downregulation of miR-652 by ARID1A, we investigated the effect of ARID1A depletion on ZFAND5 protein expression in HBE cells. As shown in Fig. 5F, silencing of ARID1A markedly suppressed the expression of ZFAND5.

ZFAND5 protects HBE cells from CSE-induced malignant transformation

Next, we investigated the role of ZFAND5 in CSE-induced malignant transformation of HBE cells. Compared to control cells, CSE-exposed HBE cells had a lower level of ZFAND5 protein (Fig. 6A). However, the level of *ZFAND5* transcript was comparable between CSE-exposed and control HBE cells (Fig. 6B). Interestingly, knockdown of ZFAND5 potentiated the proliferation, anchorage-independent growth, and migration

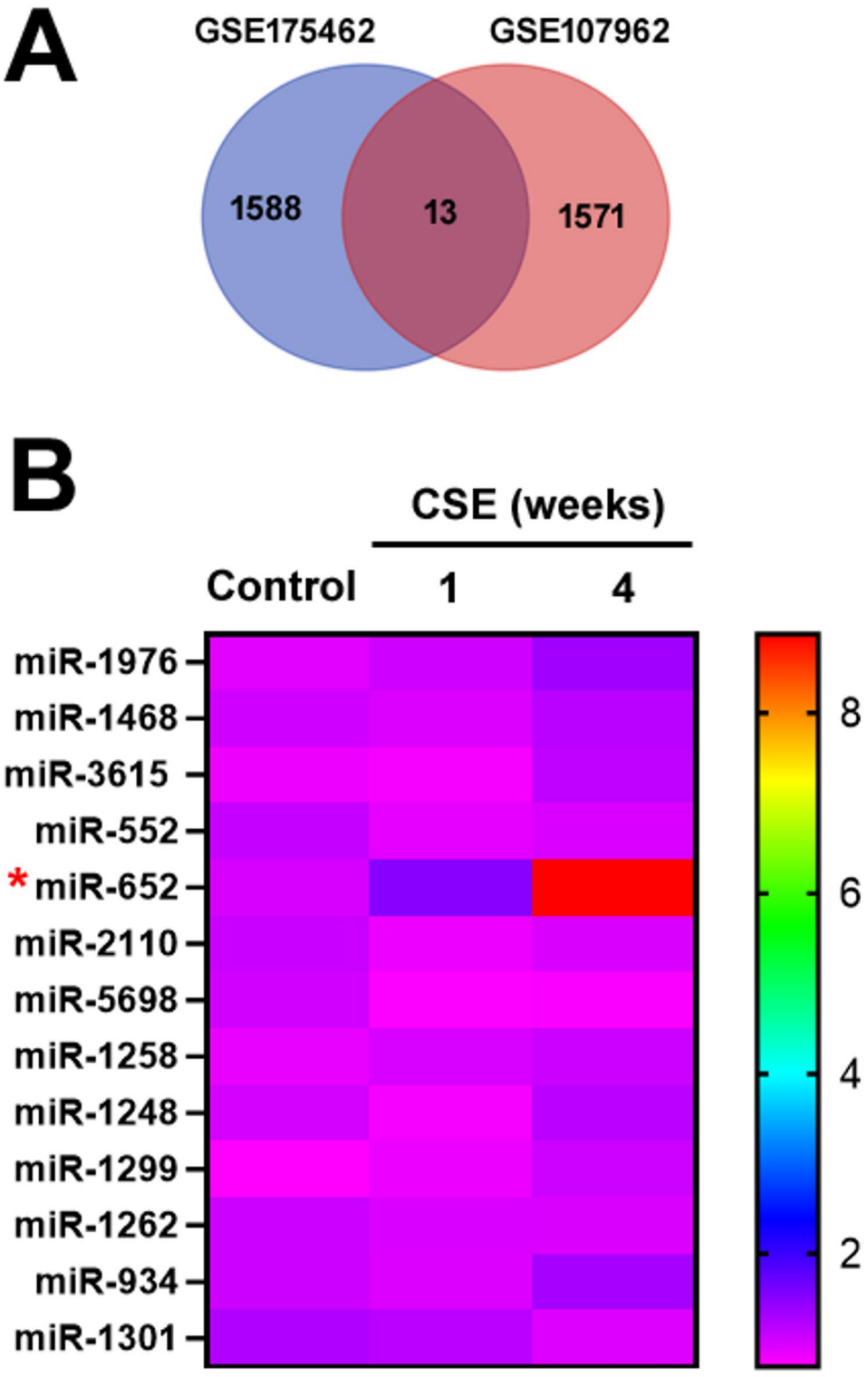

Fig. 1 miR-652 is induced in HBE cells after cigarette smoke extract (CSE) exposure. (**A**) Venn diagram depicting 13 differentially expressed miRs that were identified from 2 GEO datasets (GSE175462 and GSE107962). (**B**) Heatmap showing miR expression changes in HBE cells exposed to CSE. Asterisk (*) indicates significant difference ($P < 0.05$) between the control and CSE treatment groups ($n = 3$)

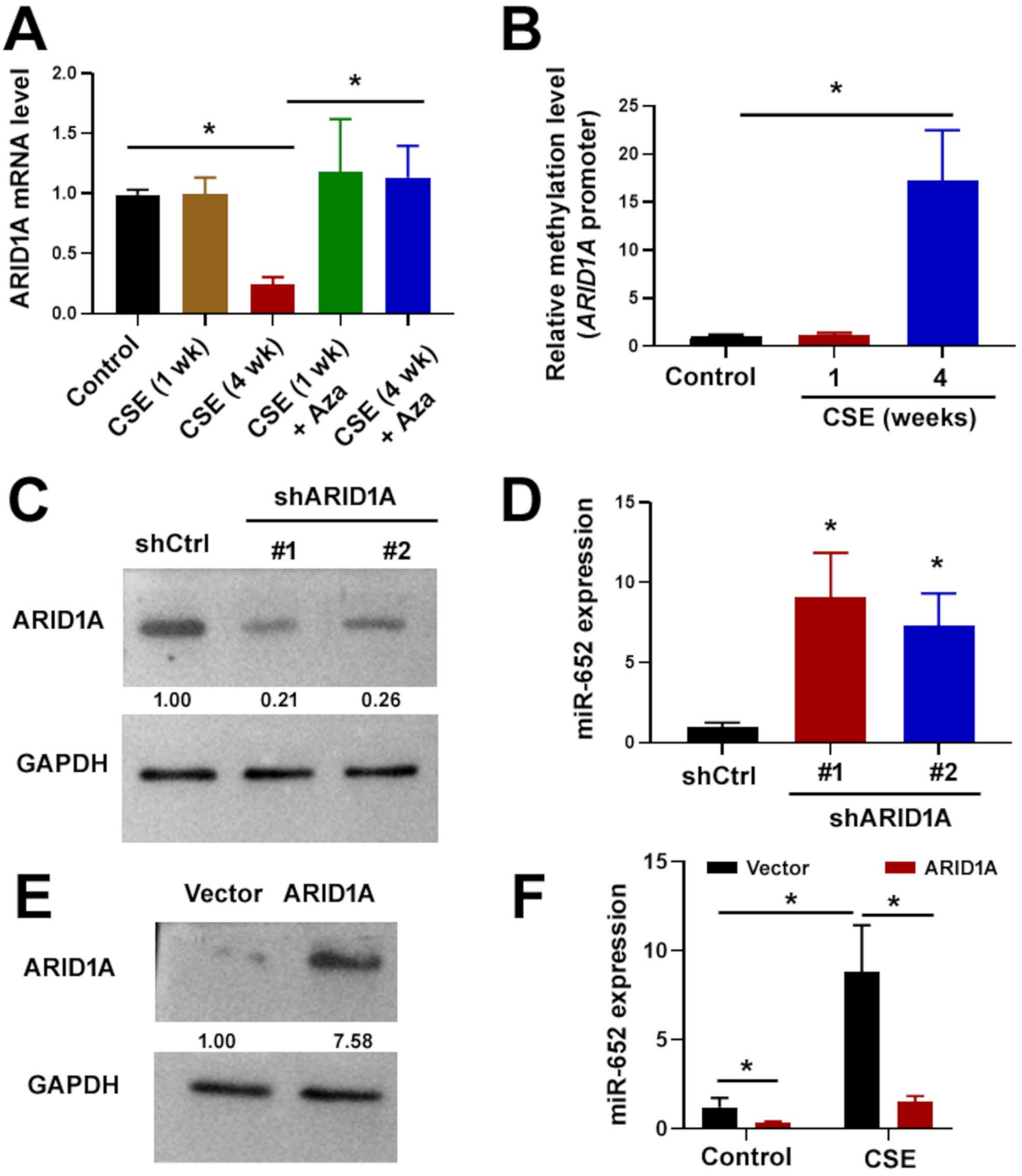

Fig. 2 Epigenetic silencing of *ARID1A* contributes to miR-652 upregulation upon cigarette smoke extract. (**A**) Measurement of ARID1A mRNA expression in different groups. 10 μM 5-azacytidine (Aza) was used to block DNA methylation. $^{*}P<0.05$ ($n=3$). (**B**) Quantification of the relative methylation level at the *ARID1A* promoter by methylated DNA immunoprecipitation assays. $^{*}P<0.05$ ($n=3$). (**C**) Western blot analysis of ARID1A protein levels in HBE cells transfected with control shRNA (shCtrl) or *ARID1A*-targeting shRNAs (shARID1A#1 and 2). Numbers below the blots represent mean densitometry ratios (normalized to the loading control) of three independent experiments. (**D**) Measurement of miR-652 levels in HBE cells transfected with indicated shRNAs. $^{*}P<0.05$ relative to the shCtrl group ($n=3$). (**E**) Western blot analysis of ARID1A protein levels. Numbers below the blots represent mean densitometry ratios (normalized to the loading control) of three independent experiments. (**F**) Overexpression of ARID1A inhibited the expression of miR-652 in HBE cells with or without 4-week CSE treatment. $^{*}P<0.05$ ($n=3$)

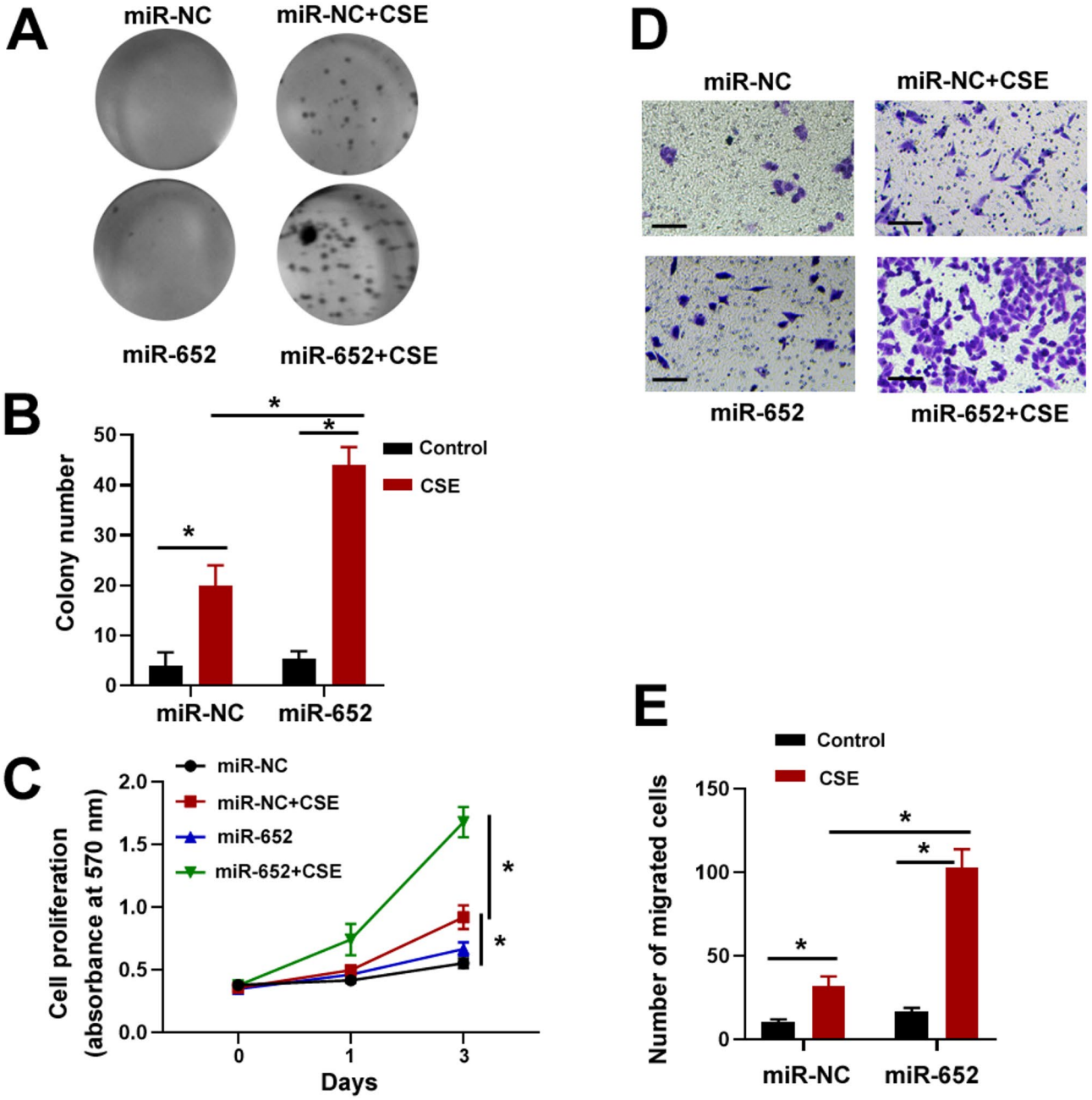

Fig. 3 miR-652 overexpression enhances CSE-induced neoplastic transformation of HBE cells. (**A**, **B**) Soft agar assays using HBE cells transfected with control miR (miR-NC) or miR-652 mimic and treated with CSE for 4 weeks. Quantification of colonies is shown in (**B**). $^{*}P < 0.05$ ($n = 3$). (**C**) Assessment of the proliferation of CSE-exposed HBE cells by the MTT assay. $^{*}P < 0.05$ ($n = 3$). (**D**, **E**) Transwell migration assay performed in CSE-exposed HBE cells. Representative images of migrated cells are shown in (**D**). Scale bar = 20 μm. Quantification of migrated cell number is shown in (**E**). $^{*}P < 0.05$ ($n = 3$)

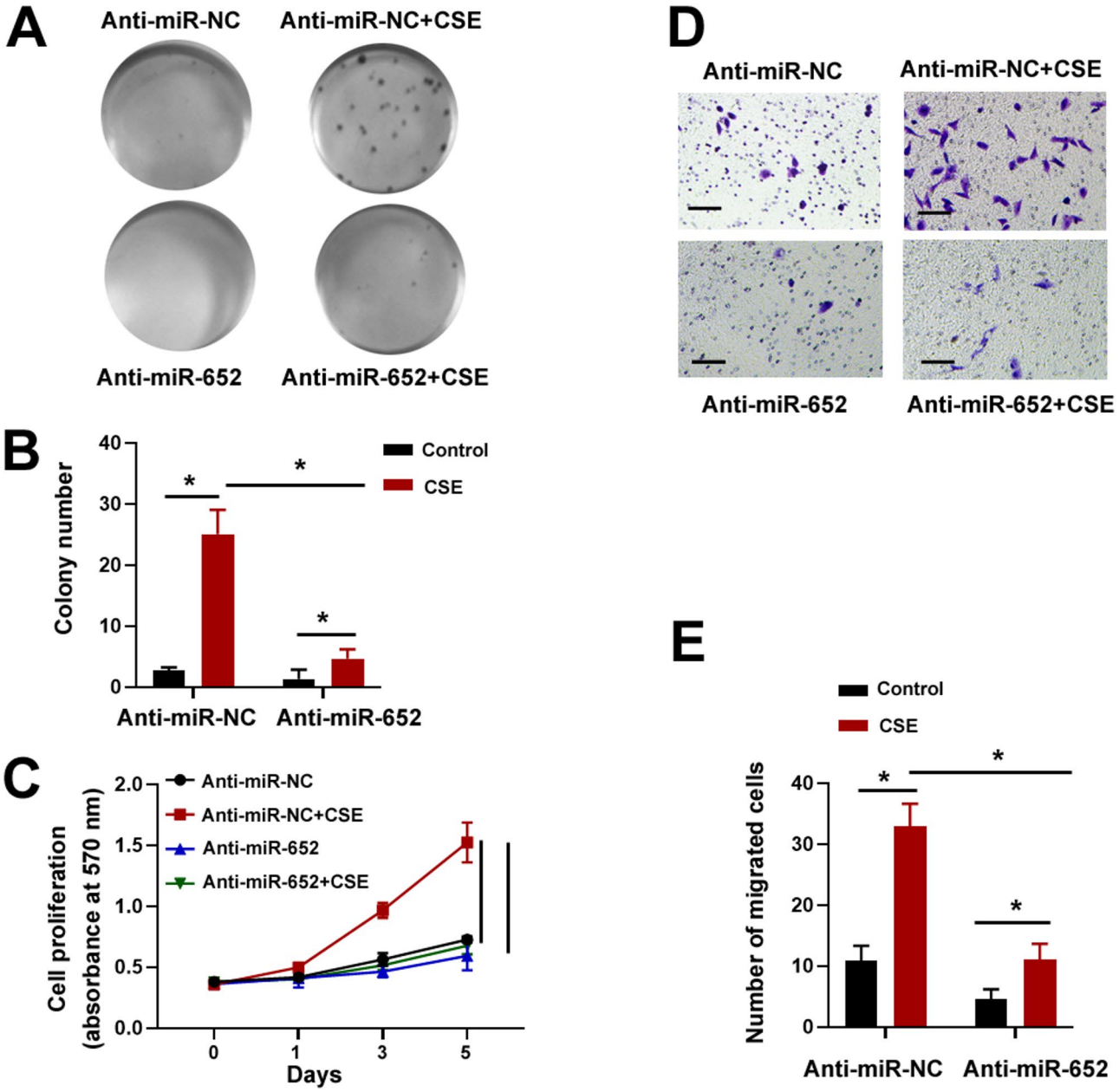

Fig. 4 Knockdown of miR-652 impairs CSE-induced aggressive phenotype in HBE cells. (**A**, **B**) Soft agar assays using HBE cells transfected with anti-miR-652 or control anti-miR (anti-miR-NC) and treated with CSE for 4 weeks. Quantification of colonies is shown in (**B**). $^{*}P < 0.05$ ($n = 3$). (**C**) Assessment of the proliferation of CSE-exposed HBE cells by the MTT assay. $^{*}P < 0.05$ ($n = 3$). (**D**, **E**) Transwell migration assay performed in CSE-exposed HBE cells. Representative images of migrated cells are shown in (**D**). Scale bar = 20 μm. Quantification of migrated cell number is shown in (**E**). $^{*}P < 0.05$ ($n = 3$)

of CSE-exposed HBE cells (Fig. 6C and G), suggesting ZFAND5 as a suppressor of HBE cell malignant transformation.

miR-652-mediated enhancement of CSE-induced aggressive phenotype in HBE cells can be rescued by overexpression of ZFAND5

Since miR-652 negatively regulates ZFAND5 expression in HBE cells, we overexpressed ZFAND5 to rescue the promoting effect of miR-652 on HBE cell malignant transformation. Western blot analysis validated the overexpression of ZFAND5 protein in HBE cells transfected with the ZFAND5-expressing plasmid (Fig. 6H). Enforced expression of ZFAND5 significantly blocked CSE-induced proliferation, anchorage-independent growth, and migration in HBE cells (Fig. 6I and K). Most importantly, the miR-652-mediated enhancement of HBE cell malignant transformation was reversed by overexpression of ZFAND5 (Fig. 6I and K). These findings support that repression of ZFAND5 is involved in

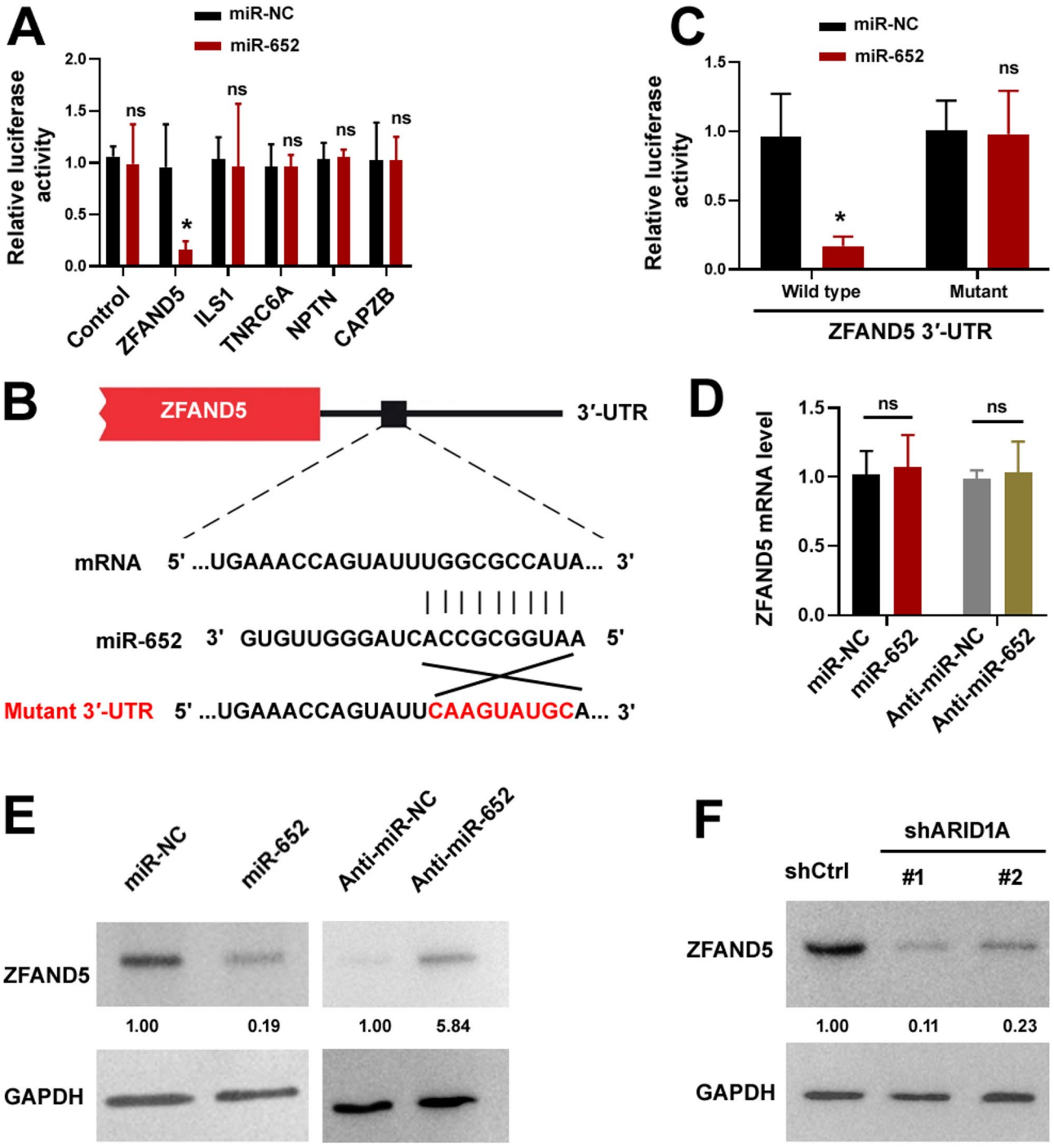

Fig. 5 miR-652 represses the protein expression of ZFAND5 in HBE cells. (**A**) Effects of miR-652 overexpression on the activities of luciferase reporters harboring the 3′-UTR of indicated mRNAs. $^{*}P < 0.05$ relative to the miR-NC group ($n = 3$). ns indicates no significance. (**B**) The predicated miR-652 binding site in the 3′-UTR of *ZFAND5*. The mutant construct showed the disruption of the miR-652 binding site. (**C**) miR-652 overexpression suppressed the luciferase reporter with the wild-type but not mutant *ZFAND5* 3′-UTR. $^{*}P < 0.05$ relative to the miR-NC group ($n = 3$). ns indicates no significance. (**D**) Measurement of *ZFAND5* mRNA levels in HBE cells transfected with miR-652 mimic, anti-miR-652 or their corresponding controls. ns indicates no significance ($n = 3$). (**E**) Western blot analysis of ZFAND5 protein levels in HBE cells transfected with miR-652 mimic, anti-miR-652 or their corresponding controls. Numbers below the blots represent mean densitometry ratios (normalized to the loading control) of three independent experiments. (**F**) Western blot analysis of ZFAND5 protein levels in HBE cells transfected with indicated shRNAs. Numbers below the blots represent mean densitometry ratios (normalized to the loading control) of three independent experiments

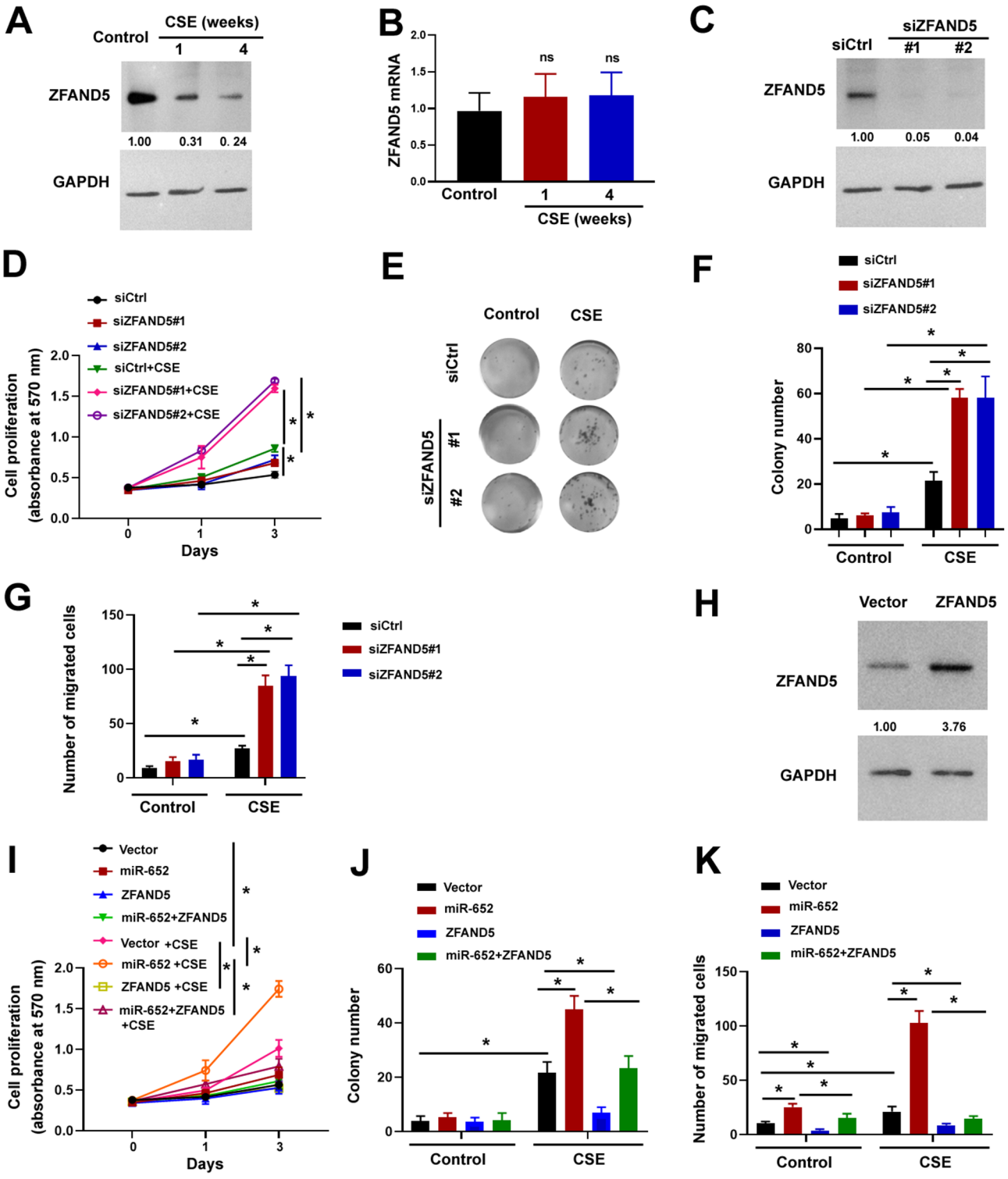

Fig. 6 (See legend on next page.)

the miR-652-mediated enhancement of aggressiveness in CSE-exposed HBE cells.

Discussion

In this work, we indicate a crucial role for miR-652 in mediating cigarette smoke-induced aggressive phenotype in HBE cells. miR-652 expression is elevated in response

(See figure on previous page.)

Fig. 6 ZFAND5 protects HBE cells from CSE-induced malignant transformation. (**A**, **B**) Measurement of ZFAND5 protein (**A**) and mRNA (**B**) levels in HBE cells with CSE treatments. ns in (**B**) indicates no significance ($n=3$). Numbers below the blots represent mean densitometry ratios (normalized to the loading control) of three independent experiments. (**C**) Western blot analysis of ZFAND5 protein levels in HBE cells transfected with control siRNA (siCtrl) or ZFAND5-targeting siRNAs. Numbers below the blots represent mean densitometry ratios (normalized to the loading control) of three independent experiments. (**D**) Assessment of the proliferation of HBE cells transfected with indicated constructs and treated with CSE for 4 weeks. $^{*}P<0.05$ ($n=3$). (**E**, **F**) HBE cells transfected with indicated constructs were exposed to CSE for 4 weeks and tested for colony formation using soft agar assays. $^{*}P<0.05$ ($n=3$). (**G**) Transwell migration assay using HBE cells transfected with indicated constructs and treated with CSE for 4 weeks. $^{*}P<0.05$ ($n=3$). (**H**) Western blot analysis of ZFAND5 protein levels in HBE cells transfected with the ZFAND5-expressing plasmid. Numbers below the blots represent mean densitometry ratios (normalized to the loading control) of three independent experiments. (**I**) Assessment of the proliferation of HBE cells transfected with indicated constructs and treated with CSE for 4 weeks. $^{*}P<0.05$ ($n=3$). (**J**) Soft agar assays using HBE cells transfected with indicated constructs and treated with CSE for 4 weeks. $^{*}P<0.05$ ($n=3$). (**K**) Transwell migration assay performed using HBE cells transfected with indicated constructs and treated with CSE for 4 weeks. $^{*}P<0.05$ ($n=3$)

to CSE treatment. Most intriguingly, enforced expression of miR-652 accelerates the proliferation, migration, and anchorage-independent growth of CSE-treated HBE cells. Depletion of miR-652 impedes the CSE-induced growth and migration of HBE cells. These results suggest that induction of miR-652 contributes to cigarette smoke-related aggressive phenotype in HBE cells.

The expression and function of miR-652 have been extensively investigated in different cancers including non-small cell lung cancer, hepatocellular carcinoma, bladder cancer, and endometrial cancer [24–27]. Elevated expression of miR-652 promotes the aggressiveness of malignant diseases. For instance, overexpression of miR-652 enhances the proliferation and invasion of hepatocellular carcinoma cells [25]. These studies indicate that miR-652 acts as an oncogenic miR to drive malignant progression. However, few studies have explored the role of miR-652 in the non-malignant context. Our data reveal that knockdown of miR-652 impairs the anchorage-independent growth and migration of CSE-treated HBE cells, highlighting importance of miR-652 in HBE cell malignant transformation. Moreover, overexpression of miR-652 can potentiate the anchorage-independent growth and migration of HBE cells after CSE exposure. However, miR-652 alone displays a mild activity to induce the growth and migration of HBE cells. In contrast, overexpression of miR-652 is sufficient to promote the proliferation and invasion of lung cancer and hepatocellular carcinoma cells [24, 25]. Thus, in the non-malignant HBE cells, the miR-652-induced malignant transformation may rely on the cooperation with other genes.

Cigarette smoke exposure causes significant changes in DNA methylation patterns in lung epithelial cells [28]. The tumor suppressor gene *NISCH* undergoes hypermethylation at its promoter region in response to cigarette smoke exposure, contributing to lung cancer development [29]. Our previous studies have reported that ARID1A acts as a tumor suppressor in lung cancer cells [20, 21]. Since ARID1A is the core component of the mammalian SWI/SNF complex, its dysregulation alters many downstream gene expression [30]. Intriguingly, we found that ARID1A has the ability to suppress the expression of miR-652 in HBE cells. Moreover, our data show that ARID1A is reduced in CSE-treated HBE cells, which is a result of hypermethylation of its promoter. Therefore, the upregulation of miR-652 in CSE-treated HBE cells can be explained by epigenetic silencing of *ARID1A*.

In different cellular contexts, miR-652 exerts its biological activities through specific target genes [24–27]. It has been reported that miR-652 targets TNRC6A to facilitate hepatocellular carcinoma metastasis and progression [25]. In bladder cancer cells, miR-652 has been found to target KCNN3 [26]. In this study, we identify ZFAND5 as a novel target for miR-652. Specially, overexpression of miR-652 decreases the expression level of ZFAND5 protein but not ZFAND5 mRNA in HBE cells, indicating a post-transcriptional regulation. Luciferase reporter assays further confirmed that miR-652-mediated repression of ZFAND5 expression relies on its binding to the 3′-UTR of *ZFAND5*. As a member of the zinc finger AN1-type domain (ZFAND) family, ZFAND5 can bind ubiquitylated substrates and thus accelerate protein degradation [31]. This gene is aberrantly expressed in several types of malignancies [32, 33]. Inhibition of ZFAND5 by miR-221-3p enhances the proliferation, invasion, and tumorigenesis in papillary thyroid carcinoma cells [33]. In the acidic microenvironment, ZFAND5 suppresses breast cancer cell growth through promotion of SLC3A2 protein degradation [34]. These studies support an important role for ZFAND5 in cancer progression. Similar to miR-652 overexpression, knockdown of ZFAND5 leads to accelerated transformation of CSE-exposed HBE cells. Moreover, enforced expression of ZFAND5 impairs the promotion of HBE cell transformation by miR-652. Our results indicate the importance of the miR-652/ZFAND5 axis in coordinating the aggressive phenotype of CSE-exposed HBE cells.

A major limitation of this study is lack of in vivo validation of the in vitro findings. It deserves to be mentioned that ARID1A loss is sufficient to drive malignant transformation of non-tumorigenic endometriotic cells [35]. Given the epigenetic silencing of *ARID1A* and subsequent induction of miR-652 in CSE-treated HBE cells,

further animal studies are needed to explore their potential to initiate neoplastic transformation of HBE cells. Additionally, the role of miR-652 in enhancing CSE-induced malignant transformation should be verified in multiple different HBE cell lines.

In conclusion, miR-652 is upregulated in CSE-treated HBE cells as a result of *ARID1A* silencing and enhances CSE-induced malignant transformation of HBE cells. Repression of ZFAND5 accounts for miR-652-mediated enhancement of HBE cell transformation upon CSE exposure. These data provide a rationale for exploring the role of miR-652 in cigarette smoke-related cancer development in animal models.

Abbreviations

CSE	Cigarette smoke extract
HBE	Human bronchial epithelial
miR	MicroRNA
qRT-PCR	Quantitative real-time PCR
shRNA	Short hairpin RNA
UTR	Untranslated region

Supplementary Information

The online version contains supplementary material available at https://doi.org/10.1186/s12890-025-03718-6.

Supplementary Material 1

Acknowledgements
None.

Author contributions
R.S.H. wrote the main manuscript text and K.L.Z. and R.S.H. validated the data. K.L.Z., D.N.W., R.H.C., C.Z., R.S.H. and X.D.Z. performed the experiments and reviewed the manuscript.

Funding
This work was supported by the Basic Scientific Research Project of Wenzhou of China (Y20220189), the Collaborative Education Project of Industry University Cooperation of the Ministry of Education of China (202101160012), and the Key Laboratory of Precision Medicine of Wenzhou of China (2021HZSY0065).

Data availability
The datasets (GSE175462 and GSE107962) used in this study are freely available from the GEO database (https://www.ncbi.nlm.nih.gov/gds/).

Declarations

Ethics approval and consent to participate
No human subjects or animals are involved in this study.

Consent for publication
Not applicable.

Competing interests
The authors declare no competing interests.

Received: 22 January 2025 / Accepted: 12 May 2025
Published online: 20 May 2025

References

1. Bouchard N, Daaboul N. Lung cancer: targeted therapy in 2025. Curr Oncol. 2025;32:146.
2. Zhang Y, Wang W, Dai K, Huang Y, Wang R, He D, He J, Liang H. Global lung cancer burden attributable to air fine particulate matter and tobacco smoke exposure: spatiotemporal patterns, sociodemographic characteristics, and transnational inequalities from 1990 to 2021. BMC Public Health. 2025;25:1260.
3. Moodie C, Best C, Critchlow N, Hitchman S, Stead M, McNeill A. The impacts of including information about the number of carcinogens in smoke on standardized cigarette packs in the UK. Eur J Public Health. 2021;31:1031–7.
4. Aggarwal RK, Sidoli S, Wang J, Sahu S, Sanawar R, Gupta V, Aluri S, Sukrithan V, Vegivinti CTR, Zavras PD, Verma D, Gordon-Mitchell S, Agarwal B, Verma T, Starczynowski DT, Steidl UG, Shastri A, Halmos B, LaFave LM, Cheng H, Verma A, Zou Y. Smoking-associated carcinogen-induced inflammation promotes lung carcinogenesis via IRAK4 activation. Clin Cancer Res. 2025;31:746–55.
5. Holland AM, Jehoul R, Vranken J, Wohl SG, Boesmans W. MicroRNA regulation of enteric nervous system development and disease. Trends Neurosci. 2025;48:268–82.
6. Razi S, Khojini JY, Norioun H, Hayati MJ, Naseri N, Tajbaksh A, Gheibihayat SM. MicroRNA-mediated regulation of ferroptosis: implications for disease pathogenesis and therapeutic interventions. Cell Signal. 2025;125:111503.
7. Zhang J, Bai R, Li M, Ye H, Wu C, Wang C, Li S, Tan L, Mai D, Li G, Pan L, Zheng Y, Su J, Ye Y, Fu Z, Zheng S, Zuo Z, Liu Z, Zhao Q, Che X, Xie D, Jia W, Zeng MS, Tan W, Chen R, Xu RH, Zheng J, Lin D. Excessive miR-25-3p maturation via N(6)-methyladenosine stimulated by cigarette smoke promotes pancreatic cancer progression. Nat Commun. 2019;10:1858.
8. Xi S, Xu H, Shan J, Tao Y, Hong JA, Inchauste S, Zhang M, Kunst TF, Mercedes L, Schrump DS. Cigarette smoke mediates epigenetic repression of miR-487b during pulmonary carcinogenesis. J Clin Invest. 2013;123:1241–61.
9. Izzotti A, Calin GA, Arrigo P, Steele VE, Croce CM, De Flora S. Downregulation of MicroRNA expression in the lungs of rats exposed to cigarette smoke. FASEB J. 2009;23:806–12.
10. Lu L, Luo F, Liu Y, Liu X, Shi L, Lu X, Liu Q. Posttranscriptional silencing of the LncRNA MALAT1 by miR-217 inhibits the epithelial-mesenchymal transition via enhancer of Zeste homolog 2 in the malignant transformation of HBE cells induced by cigarette smoke extract. Toxicol Appl Pharmacol. 2015;289:276–85.
11. Wang B, Liu Y, Luo F, Xu Y, Qin Y, Lu X, Xu W, Shi L, Liu Q, Xiang Q. Epigenetic silencing of microRNA-218 via EZH2-mediated H3K27 trimethylation is involved in malignant transformation of HBE cells induced by cigarette smoke extract. Arch Toxicol. 2016;90:449–61.
12. Zhao Y, Xu Y, Li Y, Xu W, Luo F, Wang B, Pang Y, Xiang Q, Zhou J, Wang X, Liu Q. NF-κB-mediated inflammation leading to EMT via miR-200c is involved in cell transformation induced by cigarette smoke extract. Toxicol Sci. 2013;135:265–76.
13. Bersaas A, Arnoldussen YJ, Sjøberg M, Haugen A, Mollerup S. Epithelial-mesenchymal transition and FOXA genes during tobacco smoke carcinogen induced transformation of human bronchial epithelial cells. Toxicol Vitro. 2016;35:55–65.
14. Xue J, Lv S, Yu M, Pan Y, Li N, Xu X, Zhang Q, Peng M, Liu F, Sun X, Lao Y, Yao Y, Song J, Wu J, Li B. ARID1A IDR targets EWS-FLI1 condensates and finetunes chromatin remodeling. Protein Cell. 2025;16:64–71.
15. Hartley A, Galbraith LCA, Shaw R, Tibbo A, Veeratterapillay R, Wilson L, Heer R, Blyth K, Leung H, Ahmad I. Loss of ARID1A accelerates prostate tumourigenesis with a proliferative collagen-poor phenotype through co-operation with AP1 subunit cFos. Br J Cancer. 2025;132:502–12.
16. Antoniolli M, Solovey M, Hildebrand JA, Freyholdt T, Strobl CD, Bararia D, Keay WD, Adolph L, Heide M, Passerini V, Winter L, Wange L, Enard W, Thieme S, Blum H, Rudelius M, Mergner J, Ludwig C, Bultmann S, Schmidt-Supprian M, Leonhardt H, Subklewe M, von Bergwelt-Baildon M, Colomé-Tatché M, Weigert O. ARID1A mutations protect follicular lymphoma from FAS-dependent immune surveillance by reducing RUNX3/ETS1-driven FAS-expression. Cell Death Differ. 2025. https://doi.org/10.1038/s41418-025-01445-3
17. Xu X, Padilla MT, Li B, Wells A, Kato K, Tellez C, Belinsky SA, Kim KC, Lin Y. MUC1 in macrophage: contributions to cigarette smoke-induced lung cancer. Cancer Res. 2014;74:460–70.
18. Yang S, Sun Y, Luo Y, Liu Y, Jiang M, Li J, Zhang Q, Bai J. Hypermethylation of PPARG-encoding gene promoter mediates fine particulate matter-induced pulmonary fibrosis by regulating the HMGB1/NLRP3 axis. Ecotoxicol Environ Saf. 2024;272:116068.

19. Zhang X, Sun Q, Shan M, Niu M, Liu T, Xia B, Liang X, Wei W, Sun S, Zhang Y, Liu XS, Song Q, Yang Y, Ma Y, Liu Y, Yang L, Ren Y, Zhang G, Pang D. Promoter hypermethylation of ARID1A gene is responsible for its low mRNA expression in many invasive breast cancers. PLoS ONE. 2013;8:e53931.
20. Huang R, Wu D, Zhang K, Hu G, Liu Y, Jiang Y, Wang C, Zheng Y. ARID1A loss induces P4HB to activate fibroblasts to support lung cancer cell growth, invasion, and chemoresistance. Cancer Sci. 2024;115:439–51.
21. Zheng Y, Zhang L, Zhang K, Wu S, Wang C, Huang R, Liao H. PLAU promotes growth and attenuates cisplatin chemosensitivity in ARID1A-depleted non-small cell lung cancer through interaction with TM4SF1. Biol Direct. 2024;19:7.
22. Vaz M, Hwang SY, Kagiampakis I, Phallen J, Patil A, O'Hagan HM, Murphy L, Zahnow CA, Gabrielson E, Velculescu VE, Easwaran HP, Baylin SB. Chronic cigarette smoke-induced epigenomic changes precede sensitization of bronchial epithelial cells to single-step transformation by KRAS mutations. Cancer Cell. 2017;32:360–76.
23. Xia W, Cao G, Shao N. Progress in MiRNA target prediction and identification. Sci China C Life Sci. 2009;52:1123–30.
24. Yang W, Zhou C, Luo M, Shi X, Li Y, Sun Z, Zhou F, Chen Z, He J. MiR-652-3p is upregulated in non-small cell lung cancer and promotes proliferation and metastasis by directly targeting Lgl1. Oncotarget. 2016;7:16703–15.
25. Chen W, Ru J, Wu T, Man D, Wu J, Wu L, Sun Y, Yu H, Li M, Zhang G, Zhu X, Tong R, Xiao H, Li Y, Yang B. MiR-652-3p promotes malignancy and metastasis of cancer cells via inhibiting TNRC6A in hepatocellular carcinoma. Biochem Biophys Res Commun. 2023;640:1–11.
26. Zhu QL, Zhan DM, Chong YK, Ding L, Yang YG. MiR-652-3p promotes bladder cancer migration and invasion by targeting KCNN3. Eur Rev Med Pharmacol Sci. 2019;23:8806–12.
27. Sun X, Dongol S, Qiu C, Xu Y, Sun C, Zhang Z, Yang X, Zhang Q, Kong B. miR-652 promotes tumor proliferation and metastasis by targeting RORA in endometrial Cancer. Mol Cancer Res. 2018;16:1927–39.
28. Li P, Peng J, Chen G, Chen F, Shen Y, Liu L, Chen L. DNA methylation profiling in a cigarette smoke-exposed mouse model of airway inflammation. Int J Chron Obstruct Pulmon Dis. 2022;17:2443–50.
29. Ostrow KL, Michailidi C, Guerrero-Preston R, Hoque MO, Greenberg A, Rom W, Sidransky D. Cigarette smoke induces methylation of the tumor suppressor gene NISCH. Epigenetics. 2013;8:383–8.
30. Nagarajan S, Rao SV, Sutton J, Cheeseman D, Dunn S, Papachristou EK, Prada JG, Couturier DL, Kumar S, Kishore K, Chilamakuri CSR, Glont SE, Archer Goode E, Brodie C, Guppy N, Natrajan R, Bruna A, Caldas C, Russell A, Siersbæk R, Yusa K, Chernukhin I, Carroll JS. ARID1A influences HDAC1/BRD4 activity, intrinsic proliferative capacity and breast cancer treatment response. Nat Genet. 2020;52:187–97.
31. Lee D, Zhu Y, Colson L, Wang X, Chen S, Tkacik E, Huang L, Ouyang Q, Goldberg AL, Lu Y. Molecular mechanism for activation of the 26S proteasome by ZFAND5. Mol Cell. 2023;83:2959–75.
32. Liu P, Wang Y, Duan L. ZFAND5 is an independent prognostic biomarker of Perihilar cholangiocarcinoma. Front Oncol. 2022;12:955670.
33. Hypoxic papillary thyroid, Yu F, Deng X, Zhong Y, Guo B, Zhang X, Wu B. Carcinoma cells-secreted exosomes deliver miR-221-3p to normoxic tumor cells to elicit a pro-tumoral effect by regulating the ZFAND5. Exp Cell Res. 2023;431(1):113716.
34. Xiong H, Zhai Y, Meng Y, Wu Z, Qiu A, Cai Y, Wang G, Yang L. Acidosis activates breast cancer ferroptosis through ZFAND5/SLC3A2 signaling axis and elicits M1 macrophage polarization. Cancer Lett. 2024;587:216732.
35. Lakshminarasimhan R, Andreu-Vieyra C, Lawrenson K, Duymich CE, Gayther SA, Liang G, Jones PA. Down-regulation of ARID1A is sufficient to initiate neoplastic transformation along with epigenetic reprogramming in non-tumorigenic endometriotic cells. Cancer Lett. 2017;401:11–9.

Publisher's note